Published in final edited form as:
Science. 2010 June 25; 328(5986): 1689–1693. doi:10.1126/science.1189731.

ATP-Binding Cassette Transporters and HDL Suppress Hematopoietic Stem Cell Proliferation

Laurent Yvan-Charvet[1,†,*], **Tamara Pagler**[1,*], **Emmanuel L. Gautier**[2], **Serine Avagyan**[2], **Read L. Siry**[1], **Seongah Han**[1], **Carrie L. Welch**[1], **Nan Wang**[1], **Gwendalyn J. Randolph**[2], **Hans W. Snoeck**[2], and **Alan R. Tall**[1]

[1] Division of Molecular Medicine, Department of Medicine, Columbia University, New York, NY 10032, USA

[2] Department of Gene and Cell Medicine, Mount Sinai School of Medicine, New York, NY 10029, USA

Abstract

Elevated leukocyte cell numbers (leukocytosis), and monocytes in particular, promote atherosclerosis; however, how they become increased is poorly understood. Mice deficient in the adenosine triphosphate–binding cassette (ABC) transporters ABCA1 and ABCG1, which promote cholesterol efflux from macrophages and suppress atherosclerosis in hypercholesterolemic mice, displayed leukocytosis, a transplantable myeloproliferative disorder, and a dramatic expansion of the stem and progenitor cell population containing Lin^- $Sca\text{-}1^+Kit^+$ (LSK) in the bone marrow. Transplantation of *Abca1*$^{-/-}$ *Abcg1*$^{-/-}$ bone marrow into apolipoprotein A-1 transgenic mice with elevated levels of high-density lipoprotein (HDL) suppressed the LSK population, reduced leukocytosis, reversed the myeloproliferative disorder, and accelerated atherosclerosis. The findings indicate that ABCA1, ABCG1, and HDL inhibit the proliferation of hematopoietic stem and multipotential progenitor cells and connect expansion of these populations with leukocytosis and accelerated atherosclerosis.

Leukocytosis and monocytosis are risk factors for coronary heart disease (CHD) and probably have a causal relationship to this disorder (1). In contrast, plasma high-density lipoprotein (HDL) levels are inversely correlated with the incidence of CHD (2); however, this observation has not been linked to leukocytosis. The athero-protective effect of HDL is mediated in part by promotion of cholesterol efflux from macrophage foam cells in atherosclerotic lesions (3–5). Two adenosine triphosphate–binding cassette (ABC) transporters, ABCA1 and ABCG1, play a key role in promoting cholesterol efflux from macrophages to lipid-poor apolipoprotein A-1 (apoA-1) and HDL, respectively. Deletion of *Abca1* and *Abcg1* in mice led to additive defects in macrophage cholesterol efflux and reverse cholesterol transport (6,7) and accelerated atherosclerosis in a susceptible hypercholesterolemic background (6). *Abca1*$^{-/-}$ *Abcg1*$^{-/-}$ mice also showed marked leukocytosis and infiltration of various organs with macrophage foam cells (6,8–10). This led us to hypothesize that these changes might arise, from either an inflammatory response

[†]To whom correspondence should be addressed. ly2159@columbia.edu.
[*]These authors contributed equally to this work.

Supporting Online Material
www.sciencemag.org/cgi/content/full/science.1189731/DC1
Materials and Methods
Figs. S1 to S12

mediated by excessive signaling of Toll-like receptors (TLRs) (10) or an excessive proliferation of bone marrow (BM) myeloid cells.

Six-week-old, chow-fed *Abca1*$^{-/-}$ *Abcg1*$^{-/-}$ mice developed increased myeloid cells (Gr-1^{high} CD11b^{high}), monocytosis, and neutrophilia in blood and BM (fig. S1, A and B) (11). Blood counts indicated monocytosis, neutrophilia, and eosinophilia (fig. S1C) but normal T and B cell numbers (fig. S1C) and normal hematocrit and platelet counts. Consuming a high-fat diet further increased the peripheral leukocyte and monocyte counts with a balanced increase in "inflammatory" Ly-6C^{high} and "patrolling" Ly-6C^{low} monocyte subsets in *Abca1*$^{-/-}$ *Abcg1*$^{-/-}$ mice, but not in wild-type (WT) mice (figs. S1C and S2). Besides leukocytosis, 12-week-old *Abca1*$^{-/-}$ *Abcg1*$^{-/-}$ mice fed a chow diet developed hepato-splenomegaly and hypertrophy of intestinal Peyer's patches with a cellular infiltrate of macrophage foam cells (6, 9) and neutrophils (fig. S3).

To determine if leukocytosis in *Abca1*$^{-/-}$ *Abcg1*$^{-/-}$ mice might represent an inflammatory response, we bred *Abca1*$^{-/-}$ *Abcg1*$^{-/-}$ to *MyD88*$^{-/-}$ mice, which lack the adapter molecule MyD88 necessary for signaling downstream of some TLRs. These animals showed only slight reductions in leukocyte and neutrophil counts compared with *Abca1*$^{-/-}$ *Abcg1*$^{-/-}$ mice, although spleen weight was similar (fig. S4, A and B). Furthermore, treatment of *Abca1*$^{-/-}$ *Abcg1*$^{-/-}$ mice with broad spectrum antibiotics to suppress potential TLR-dependent responses to the endogenous intestinal flora (12) did not reverse leukocytosis or splenomegaly in *Abca1*$^{-/-}$ *Abcg1*$^{-/-}$ mice (fig. S4, C and D). These findings were inconsistent with the hypothesis that leukocytosis represented a TLR/MyD88-dependent inflammatory response.

The phenotype of the *Abca1*$^{-/-}$ *Abcg1*$^{-/-}$ mice suggested a myeloproliferative disorder, and both ABCA1 and ABCG1 are highly expressed in hematopoietic stem and multipotential progenitor cells (HSPCs) (13,14). Thus, we quantified BM HSPCs and other myeloid populations in chow-fed animals (Fig. 1) (15). Remarkably, the Lin^{-} Sca^{+}cKit^{+} (LSK) population representing HSPCs showed a fivefold increase in both frequency and number in *Abca1*$^{-/-}$ *Abcg1*$^{-/-}$ BM (Fig. 1A and fig. S5, A to D). Although the common lymphoid progenitor (CLP) population was unchanged, the granulocyte-monocyte progenitor (GMP) and the common myeloid progenitor (CMP) numbers were increased up to 100% in *Abca1*$^{-/-}$ *Abcg1*$^{-/-}$ BM compared with WT BM (Fig. 1A and fig. S5, E and F). Analysis of different populations within the LSK cells showed that CD34^{+}CD150^{-} CD135^{-} multipotential progenitors were increased as a percentage of the LSK population (Fig. 1, B and C). However, because the overall LSK population was increased fivefold (Fig. 1A), all CD34^{+} cells were expanded as a percentage of total BM cells (Fig. 1C), including short-term hematopoietic stem cells (HSCs) (CD34^{+}CD150^{+}CD135^{-}) and both populations of CD34^{+} multipotential progenitors (15,16). However, CD34^{-} CD150^{+}CD135^{-} long-term HSCs were not increased. The expansion of myeloid progenitors and LSK cells in double-knockout BM reflected an increase in cell cycling. In *Abca1*$^{-/-}$ *Abcg1*$^{-/-}$ mice, there was a threefold increase in the SG2M fraction in total BM cells (fig. S5G) and a fivefold increase in the SG2M fraction in LSK cells compared with controls (Fig. 1D and fig. S5H). Colony-forming assays also confirmed an approximately twofold increase in the number and size of granulocyte/macrophage colony-forming units (GM-CFUs) for all of the growth factors tested in *Abca1*$^{-/-}$ *Abcg1*$^{-/-}$ compared with WT cultures (Fig. 2, A and B, and fig. S6A).

To test whether this phenotype was caused by cell autonomous effects of ABCA1 and ABCG1 within the hematopoietic system or an effect of the microenvironment, we mixed BM cells from CD45.1 WT mice with CD45.2 *Abca1*$^{-/-}$ *Abcg1*$^{-/-}$ BM in vitro. CD45.1 WT BM cell proliferation was not affected by the presence of CD45.2 *Abca1*$^{-/-}$ *Abcg1*$^{-/-}$ cells, confirming a cell autonomous effect (fig. S6B). The competitive advantage of *Abca1*$^{-/-}$

Abcg1$^{-/-}$ cells was also shown in a BM transplantation experiment with similar mixed donor-cell populations (fig. S7).

We next investigated the relation of BM myeloid proliferation to HDL-mediated cholesterol efflux. HDL markedly reduced the number and size of GM-CFUs from *Abca1*$^{-/-}$ *Abcg1*$^{-/-}$ mice and also reduced the size of the GM-CFUs from WT mice (Fig. 2A and fig. S6A). Consistent with these findings, HDL also decreased the proliferation rates of interleukin-3 (IL-3) and granulocyte macrophage colony-stimulating factor (GM-CSF)–treated WT and *Abca1*$^{-/-}$ *Abcg1*$^{-/-}$ BM cells in a dose-dependent fashion, but *Abca1*$^{-/-}$ *Abcg1*$^{-/-}$ cells showed smaller responses to HDL, in terms of both proliferation and cholesterol efflux (fig. S8, A and B). Whereas lipid-poor apoA-1 had no effect on proliferation of *Abca1*$^{-/-}$ *Abcg1*$^{-/-}$ cells, mouse plasma HDL showed a similar suppression of proliferation, and this was greater for apoA-1 transgenic plasma HDL compared with control HDL (fig. S8C). These results suggest that HDL suppresses the proliferation of myeloid progenitor cells by promoting cholesterol efflux. This effect is still observed in *Abca1*$^{-/-}$ *Abcg1*$^{-/-}$ BM, possibly reflecting the ability of HDL to promote cholesterol efflux by alternative pathways such as passive or diffusional cholesterol efflux (17). Single-knockout deficiency revealed only a slight increase in proliferation for *Abca1*$^{-/-}$ cultures and no effect for *Abcg1*$^{-/-}$ cultures (fig. S8D), consistent with the synergistic role of these transporters in mediating cellular cholesterol efflux (6). Although liver X receptor (LXR) transcription factors induce expression of both *Abca1* and *Abcg1,* and LXR knockout mice have increased lymphocyte proliferation (18), we did not observe any increase in T or B cells in blood (fig. S1C), spleen, or lymph nodes in *Abca1*$^{-/-}$ *Abcg1*$^{-/-}$ mice. Expansion of myeloid populations was not reported in LXRα/β$^{-/-}$ mice (18), possibly due to their relatively high levels of basal *Abca1* and *Abcg1* expression (19). Treatment of BM myeloid cells with an LXR activator (TO901317), however, resulted in increased cholesterol efflux and decreased growth factor–stimulated proliferation in WT (but not *Abca1*$^{-/-}$ Abcg1$^{-/-}$) cells (fig. S9, A and B). This indicates that activation of LXR induced *Abca1* and *Abcg1*, promoting cholesterol efflux and suppressing proliferation. Conversely, stimulation of WT BM myeloid cell proliferation with IL-3 or GM-CSF markedly reduced the expression of these transporters (fig. S9, C and D).

ApoA-1 transgenic mice have increased apoA-1 and HDL levels and are resistant to atherosclerosis (20,21). To examine whether HDL could suppress myeloproliferation in vivo, we transplanted BM from WT and *Abca1*$^{-/-}$ *Abcg1*$^{-/-}$ mice into chow-fed normocholesterolemic WT or apoA-1 transgenic recipients. We observed a dramatic decrease in the frequency, numbers, and cycling activity of the LSK population and a reversal of the splenomegaly in apoA-1 transgenic recipients of *Abca1*$^{-/-}$ *Abcg1*$^{-/-}$ BM, but not in WT recipients (Fig. 2, B to D, and fig. S9E). The increased proliferation of *Abca1*$^{-/-}$ *Abcg1*$^{-/-}$ LSK cells was associated with increased cholera toxin subunit B (CTx-B) staining of the cell surface of *Abca1*$^{-/-}$ *Abcg1*$^{-/-}$ compared with WT LSK cells (fig. S9F), suggesting increased formation of cholesterol-rich lipid rafts (22,23). This staining was decreased in LSK cells isolated from apoA-1 transgenic mice transplanted with WT or *Abca1*$^{-/-}$ *Abcg1*$^{-/-}$ BM (fig. S9F). In vitro treatment of *Abca1*$^{-/-}$ *Abcg1*$^{-/-}$ LSK cells with cyclodextrin, which mediates cholesterol efflux and reduces lipid raft formation, also led to markedly decreased CTx-B staining (fig. S9G).

To identify the underlying mechanisms responsible for the myeloproliferative phenotype, we cultured BM cells in the presence of different growth factors known to induce the proliferation of HSCs. Although stem cell factor (SCF or kit-ligand) increased the percentage of bromodeoxyuridine (BrdU, used to measure proliferating cells)–positive cells in BM or LSK cells, there was no significant difference in response between the genotypes (Fig. 3, A and B). In contrast, both IL-3 and GM-CSF significantly increased the percentage

of BrdU-positive cells in *Abca1*$^{-/-}$ *Abcg1*$^{-/-}$ BM and LSK cells. Consistent with these findings, increased activation of phospo–extracellular signal–regulated kinase (ERK) in response to IL-3 and GM-CSF treatments was observed in both *Abca1*$^{-/-}$ *Abcg1*$^{-/-}$ BM and LSK cells in vivo (Fig. 3C) and in response to IL-3 and GM-CSF in cell culture (Fig. 3D). Increased phospho-ERK was associated with increased Ras protein in the plasma membrane of *Abca1*$^{-/-}$ *Abcg1*$^{-/-}$ BM myeloid cells and increased Ras guanosine triphosphatase activity; these changes were reversed by HDL treatment (Fig. 3E). Treatment with cyclodextrin or with a farnesyl transferase inhibitor known to prevent the anchorage of Ras in the plasma membrane also caused a marked reduction in proliferation of WT and *Abca1*$^{-/-}$ *Abcg1*$^{-/-}$ BM cells (fig. S10, A and B). The IL-3 and GM-CSF receptors share a common β subunit (24, 25). The number of cells expressing the IL-3 receptor β subunit at the cell surface was increased twofold in *Abca1*$^{-/-}$ *Abcg1*$^{-/-}$ BM cells and fivefold in *Abca1*$^{-/-}$ *Abcg1*$^{-/-}$ LSK cells; this was reversed in the presence of the apoA-1 transgene (Fig. 3, F to H). Other potential mechanisms to explain increased numbers of *Abca1*$^{-/-}$ *Abcg1*$^{-/-}$ BM myeloid cells were also investigated, such as decreased apoptosis, oxidative stress, or increased TLR- or wnt-dependent signaling. Although the small decrease in numbers of apoptotic cells observed in the basal state might also contribute to the increased number of myeloid cells (fig. S10C), neither lack of Myd88 or antioxidant treatment was able to reduce the enhanced proliferation rates of *Abca1*$^{-/-}$ *Abcg1*$^{-/-}$ BM myeloid cells (fig. S10, D to F). mRNA expression analysis of GM-CSF colony-forming cells also did not reveal up-regulation of the canonical wnt signaling target genes Axin1 and Axin2 or changes in the key transcriptional factors C/EBPα and ε known to regulate both the proliferation and differentiation of myeloid progenitors in contrast to increased phospho-Erk target gene expression such as c-jun and cyclin D1 (fig. S11). Consistent with the proposed mechanism, we also found an increase in PU.1, a key transcription factor that promotes development of myeloid lineages, including monocytes and neutrophil lineages (26). Together, these data suggest that increased membrane cholesterol content secondary to ABC transporter deficiency results in increased cell-surface expression of the common β subunit of the IL-3/GM-CSF receptor that, in turn, leads to increased downstream Ras/Erk signaling and increased proliferative responses to IL-3 and GM-CSF.

To investigate whether the apoA-1 transgene could suppress the myeloproliferative phenotype and accelerated atherosclerosis of hypercholesterolemic *Abca1*$^{-/-}$ Abcg1$^{-/-}$ mice, we also transplanted BM from WT and *Abca1*$^{-/-}$ *Abcg1*$^{-/-}$ mice into high cholesterol–fed, atherosclerosis-susceptible *Ldlr*$^{+/-}$ mice with or without the human apoA-1 transgene. HDL cholesterol and human apoA-I levels were similar in the two groups of mice (fig. S12, A and B). Remarkably, the myeloid cell infiltration of different organs in *Abca1*$^{-/-}$ *Abcg1*$^{-/-}$ BM recipients was almost completely suppressed by expression of the human apoA-1 transgene (Fig. 4, A to C). There was marked reduction of splenomegaly with normalization of the hypercellularity (Fig. 4A). The livers that had a nutmeg appearance became normal, and the hypertrophied Peyer's patches (Fig. 4C) disappeared. The small, pale hearts infiltrated with neutrophils and foam cells were replaced with normal-sized hearts without cellular infiltration (Fig. 4B). The apoA-I transgene also dramatically suppressed the accelerated atherosclerosis in atherogenic diet–fed *Ldlr*$^{+/-}$ mice receiving *Abca1*$^{-/-}$ *Abcg1*$^{-/-}$ BM (Fig. 4, D and E). In *Abca1*$^{-/-}$ *Abcg1*$^{-/-}$ BM recipients, the extent of atherosclerosis was correlated with the degree of leukocytosis (Fig. 4D), and leukocytosis was suppressed by the apoA-1 transgene (Fig. 4F). A serum inflammatory marker, apoSAA, was also suppressed by the apoA-1 transgene in *Abca1*$^{-/-}$ *Abcg1*$^{-/-}$ mice, but there was no correlation between levels of apoSAA and the extent of atherosclerosis (fig. S12, C and D).

Collectively, our results suggest that proliferation of HSPCs is normally regulated by cholesterol efflux mechanisms involving LXRs, ABCA1, ABCG1, and HDL. Our studies also suggest a previously unsuspected role of HSPC proliferation in the leukocytosis of

atherosclerosis and reveal that HDL can exert an anti-atherogenic effect by suppressing this proliferation. Hypercholesterolemia and high-fat feeding in different species results in leukocytosis and monocytosis (27–30) and increased entry of monocytes into atherosclerotic lesions (28–30). Although monocytosis is insufficient to induce atherosclerosis, lesion burden is directly proportional to monocyte counts in the blood (31). Our studies indicate a link between expansion of HSPCs, leukocytosis, and accelerated atherosclerosis in *Abca1*$^{-/-}$ *Abcg1*$^{-/-}$ mice. The apoA-1 transgene significantly reduced leukocytosis in hypercholesterolemic *Ldlr*$^{+/-}$ mice receiving WT BM (Fig. 4F), suggesting a general role for HDL in the suppression of HSPC proliferation in hypercholesterolemic animal models. Although increasing HDL levels may reduce atherosclerosis by several different mechanisms, our findings suggest that the suppression of BM myeloid proliferation, leukocytosis, and monocytosis might represent a previously unidentified anti-atherogenic effect of HDL acting at an earlier stage in the leukocyte life cycle than subsequent anti-inflammatory or antioxidant effects occurring in the vessel wall (3–5). This property might also find an application in the treatment of myeloproliferative disorders.

Supplementary Material

Refer to Web version on PubMed Central for supplementary material.

Acknowledgments

This work is supported by a Program Project grant from the NIH to A.R.T. (HL54591) and a grant from the American Heart Association to L.Y.-C. (SDG2160053), by the FWF Austrian Science Fund (T.P.), and by NIH grants R01A1061741 (E.L.G. and G.J.R.) and R01AG016327 (H.W.S.). A.R.T. serves on scientific advisory boards for Merck and Arisaph Pharmaceuticals and provides paid consulting services to Roche, Merck, Arisaph Pharmaceuticals, and CSL Limited related to the development of drugs that would increase HDL levels.

References and Notes

1. Coller BS. Arterioscler Thromb Vasc Biol 2005;25:658. [PubMed: 15662026]
2. Gordon DJ, Rifkind BM. N Engl J Med 1989;321:1311. [PubMed: 2677733]
3. Barter PJ, Puranik R, Rye KA. Curr Cardiol Rep 2007;9:493. [PubMed: 17999875]
4. Tall AR, Yvan-Charvet L, Terasaka N, Pagler T, Wang N. Cell Metab 2008;7:365. [PubMed: 18460328]
5. Duffy D, Rader DJ. Nat Rev Cardiol 2009;6:455. [PubMed: 19488077]
6. Yvan-Charvet L, et al. J Clin Invest 2007;117:3900. [PubMed: 17992262]
7. Wang X, et al. J Clin Invest 2007;117:2216. [PubMed: 17657311]
8. Out R, et al. Arterioscler Thromb Vasc Biol 2008;28:258. [PubMed: 18006857]
9. Out R, et al. Circ Res 2008;102:113. [PubMed: 17967783]
10. Yvan-Charvet L, et al. Circulation 2008;118:1837. [PubMed: 18852364]
11. Materials and methods are available as supporting material on *Science* Online.
12. Turer EE, et al. J Exp Med 2008;205:451. [PubMed: 18268035]
13. Peeters SD, et al. Exp Hematol 2006;34:622. [PubMed: 16647568]
14. de Grouw EP, et al. Leukemia 2006;20:750. [PubMed: 16467867]
15. Weissman IL, Shizuru JA. Blood 2008;112:3543. [PubMed: 18948588]
16. Wilson A, et al. Cell 2008;135:1118. [PubMed: 19062086]
17. Adorni MP, et al. J Lipid Res 2007;48:2453. [PubMed: 17761631]
18. Bensinger SJ, et al. Cell 2008;134:97. [PubMed: 18614014]
19. Wagner BL, et al. Mol Cell Biol 2003;23:5780. [PubMed: 12897148]
20. Rubin EM, Krauss RM, Spangler EA, Verstuyft JG, Clift SM. Nature 1991;353:265. [PubMed: 1910153]

21. Plump AS, Scott CJ, Breslow JL. Proc Natl Acad Sci USA 1994;91:9607. [PubMed: 7937814]
22. Dietrich C, Volovyk ZN, Levi M, Thompson NL, Jacobson K. Proc Natl Acad Sci USA 2001;98:10642. [PubMed: 11535814]
23. Nichols BJ. Curr Biol 2003;13:686. [PubMed: 12699627]
24. Chang F, et al. Leukemia 2003;17:1263. [PubMed: 12835716]
25. Testa U, et al. Leukemia 2004;18:219. [PubMed: 14671644]
26. Geissmann F, et al. Science 2010;327:656. [PubMed: 20133564]
27. Averill LE, Meagher RC, Gerrity RG. Am J Pathol 1989;135:369. [PubMed: 2675618]
28. Swirski FK, et al. Proc Natl Acad Sci USA 2006;103:10340. [PubMed: 16801531]
29. Swirski FK, et al. J Clin Invest 2007;117:195. [PubMed: 17200719]
30. Tacke F, et al. J Clin Invest 2007;117:185. [PubMed: 17200718]
31. Combadière C, et al. Circulation 2008;117:1649. [PubMed: 18347211]

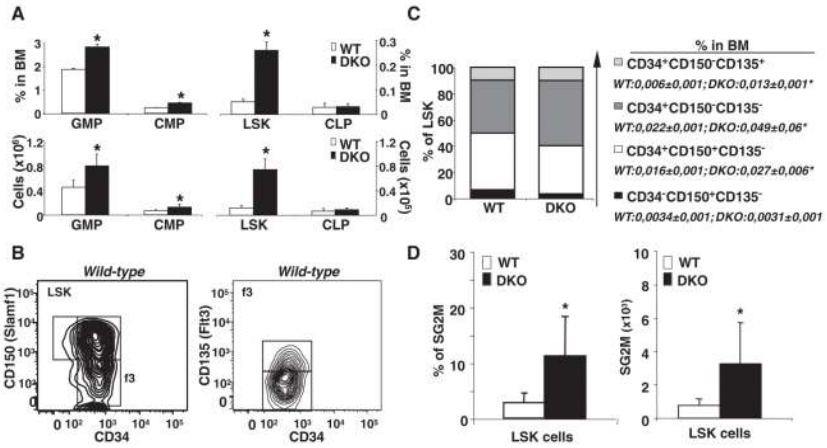

Fig. 1.

Increased expansion and cycling activity of nontransplanted Abca1$^{-/-}$ Abcg1$^{-/-}$ HSCs. (**A**) Quantification of LSK, CMP, GMP, and CLP compartments expressed as percentage of total BM or absolute numbers. DKO, double knockout. (**B**) Using flow cytometric analysis, LSK populations were subdivided into four populations based on differential expression of CD34 and CD150, and CD135 (Flt3) represents gated CD34^{+} CD150^{-} LSK cells. (**C**) Quantification of LSK subpopulations from the most quiescent (long-term HSCs) to the most cycling LSK subset (short-term HSCs and multipotential progenitors) (CD34^{-} CD150^{+} CD135^{-} > CD34^{+} CD150^{+} CD135^{-} > CD34^{+} CD150^{-} CD135^{-} > CD34^{+} CD150^{-} CD135^{+}) expressed as percentage of LSK population or whole BM. (**D**) Percentage and absolute number of LSK cells in S/G2M phase as determined by Hoechst staining and flow cytometric analysis. Data are means ± SEM (error bars) and are representatives of at least one experiment performed with five animals per group. *$P < 0.05$.

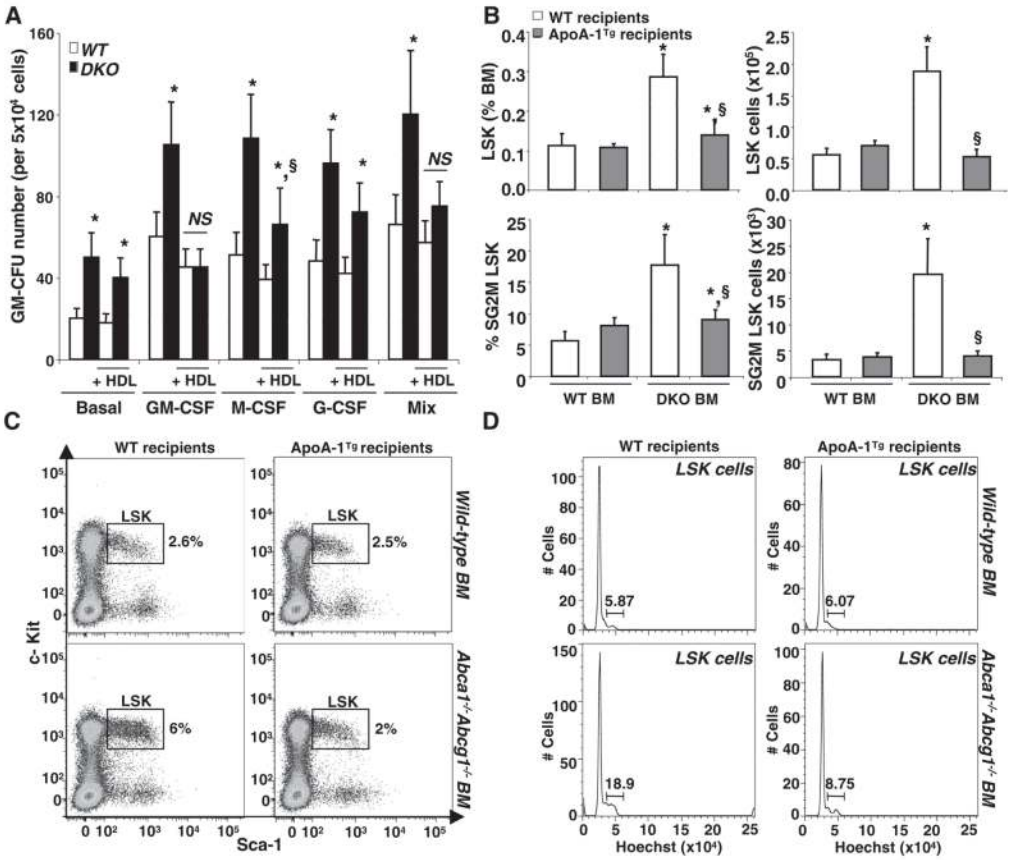

Fig. 2.

HDL prevents HSCs from entry into the cell cycle. (**A**) Colony-forming assay using control and *Abca1*$^{-/-}$ *Abcg1*$^{-/-}$ BM was performed in presence or absence of 50 μg/mL HDL cholesterol. GM-CFU numbers induced by indicated growth factors alone or in combination (Mix) were determined from methylcellulose dishes after 10 days in culture. Results are ± SEM (error bars) of four mice per experimental group. (**B**) Quantification and (**C**) representative dot plots of LSK in chow-fed WT and apoA-I transgenic recipient mice transplanted with control or Abca1$^{-/-}$ Abcg1$^{-/-}$ BM. (**D**) Comparison of the cell cycle of LSK cells by flow cytometric analysis of Hoechst staining. Data are means ± SEM of five to six animals per group. *P < 0.05 genotype effect; §P < 0.05 treatment effect.

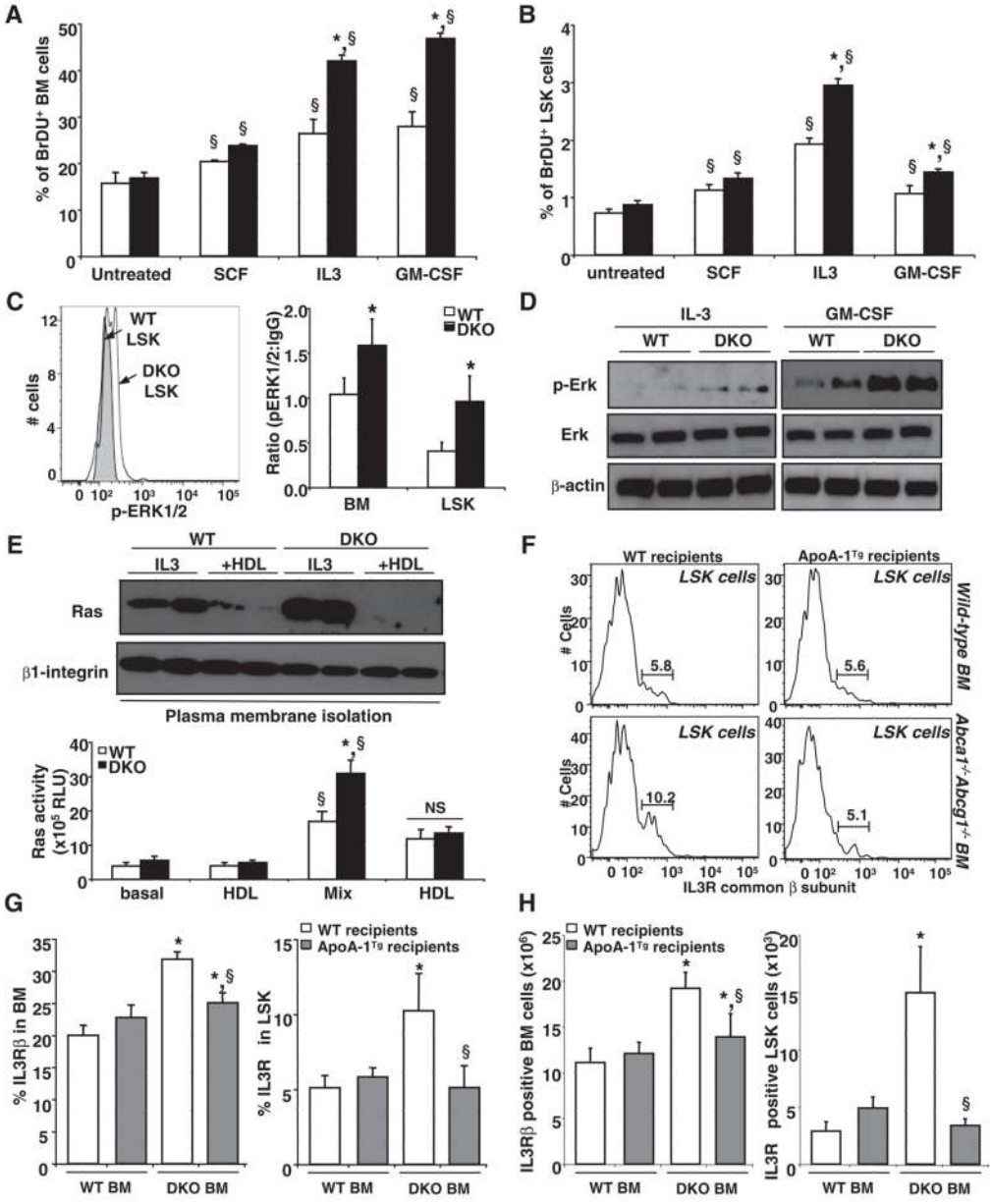

Fig. 3.

HDL protects myeloid cells from activation of IL-3–receptor β canonical pathway. (**A**) WT and *Abca1*$^{-/-}$ *Abcg1*$^{-/-}$ BM cells and (**B**) LSK cells were grown for 72 hours in liquid culture in the presence of indicated growth factors and were analyzed for BrdU incorporation by flow cytometry. (**C**) Representative histogram and bar graph showing the expression of phoshpERK1/2 by flow cytometry in freshly isolated BM and LSK cells from WT mice transplanted with control or *Abca1*$^{-/-}$ *Abcg1*$^{-/-}$ BM. (**D**) Western blot analysis shows phospho-ERK, total ERK, and β-actin expression in WT and *Abca1*$^{-/-}$ *Abcg1*$^{-/-}$ BM cells treated with indicated growth factors in duplicate samples. (**E**) Duplicate samples of BM cells treated with indicated growth factors and 50 μg/mL HDL cholesterol were subjected to plasma membrane fractionation and analyzed for Ras and β1-integrin expression or used to quantify Ras activity. (**F**) Representative histograms showing the expression of the IL-3–receptor β in LSK cells from WT and apoA-I transgenic recipient

mice transplanted with control or *Abca1*$^{-/-}$ *Abcg1*$^{-/-}$ BM. (**G**) Percentage and (**H**) absolute number of BM and LSK cells expressing the IL-3Rβ are depicted from the above-mentioned mice. Results are means ± SEM (error bars) of five to six mice per group. *$P < 0.05$ genotype effect; §$P < 0.05$ treatment effect.

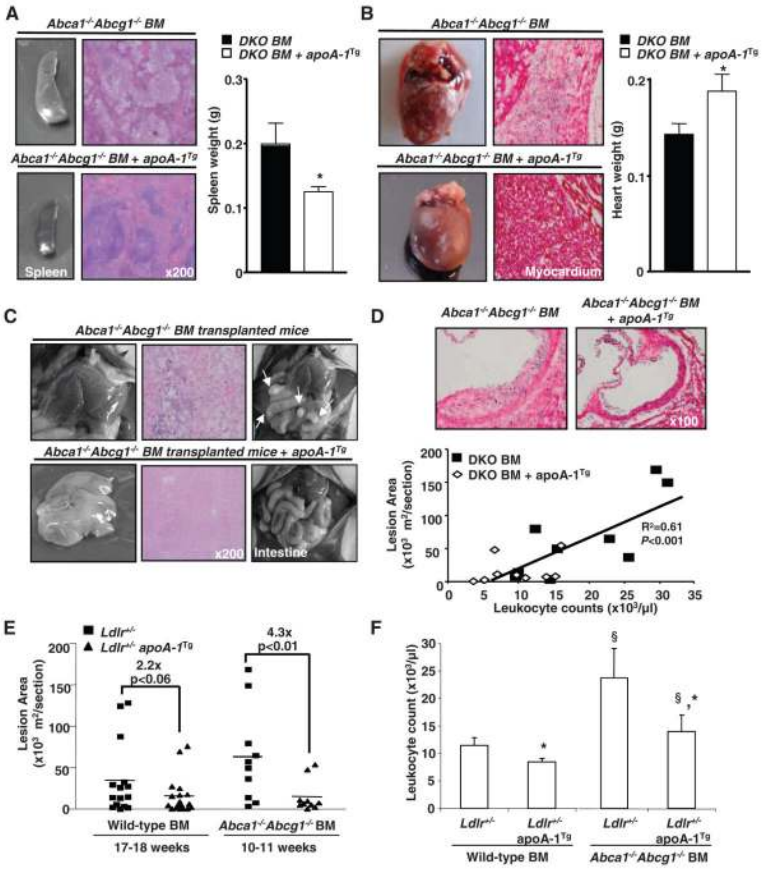

Fig. 4.

HDL rescue the myeloproliferative disorder and accelerated atherosclerosis of *Abca1*$^{-/-}$ *Abcg1*$^{-/-}$ BM transplanted mice. (**A**) Representative spleen, (**B**) heart, (**C**) liver, Peyer's patches, and hematoxylin and eosin (H&E) staining of paraffin-embedded sections from high cholesterol–fed *Ldlr*$^{+/-}$ and *Ldlr*$^{+/-}$ apoA-1 transgenic recipient mice transplanted with *Abca1*$^{-/-}$ *Abcg1*$^{-/-}$ BM. (**D**) Representative H&E staining of the proximal aortas showing atherosclerotic lesions and correlation between mean lesion areas and leukocyte counts. (**E**) Lesion areas (individual and mean) were determined by morphometric analysis of H&E-stained sections. BM transplanted mice were fed a high-cholesterol diet for different time periods to approximately match lesion areas for mice not expressing apoA-1 transgene. (**F**) Leukocyte counts from WT and *Abca1*$^{-/-}$ *Abcg1*$^{-/-}$ transplanted recipients. Results are means ± SEM (error bars) of six to nine mice per group. **P* < 0.05 apoA-I transgene effect; §*P* < 0.05 BM transplant effect.